Acta Cryst. (1999). A**55**, 14–19

Temperature-dependent X-ray dynamical diffraction: Darwin theory simulations

Jin-Seok Chung and Stephen M. Durbin*

Department of Physics, Purdue University, West Lafayette, IN 47907-1396, USA. E-mail: durbin@physics.purdue.edu

(*Received 22 September 1997; accepted 15 May 1998*)

Abstract

Thermal vibrations destroy the perfect crystalline periodicity generally assumed by dynamical diffraction theories. This can lead to some difficulty in deriving the temperature dependence of X-ray reflectivity from otherwise perfect crystals. This difficulty is overcome here in numerical simulations based on the extended Darwin theory, which does not require periodicity. Using Si and Ge as model materials, it is shown how to map the lattice vibrations derived from measured phonon dispersion curves onto a suitable Darwin model. Good agreement is observed with the usual Debye–Waller behavior predicted by standard theories, except at high temperatures for high-order reflections. These deviations are discussed in terms of a possible breakdown of the ergodic hypothesis for X-ray diffraction.

1. Introduction

Thermal vibrations present a peculiar problem for X-ray dynamical diffraction: the theory is based on a crystal with perfect periodicity, yet lattice vibrations destroy this very periodicity. Nonetheless, various arguments have been put forward suggesting that the Bragg intensity temperature dependence caused by thermal vibrations should have an $\exp[-M(T)]$ temperature dependence, where $M(T)$ is the usual Debye factor proportional to the mean vibrational amplitude (James, 1950; Batterman & Cole, 1964). [This is in contrast to the $\exp(-2M)$ seen in kinematically diffracting crystals.] This behavior is observed experimentally (Batterman, 1962), and there has been some theoretical justification for it (Parthasarathy, 1960; Ohtsuki, 1964). In this work, we present numerical simulations which largely support this conclusion but which also indicate significant deviations from Debye behavior at high temperatures and short interplanar spacings. This raises some questions about the underlying assumptions of the Debye picture of scattering from the time-averaged charge distribution of the crystal.

This work is based on the Darwin theory. While most descriptions of X-ray dynamical diffraction begin with the von Laue picture of a crystal as a periodic dielectric medium, the original Darwin theory computes the reflectivity from a regular stack of identical atomic planes. Darwin's derivation begins with the reflectivity of a single atomic plane and, by assuming a perfect array of these, is able to deduce an analytical expression for what is now known as the Darwin reflectivity curve. More recently, it has been shown that realistic non-periodic structures can be simulated by simply computing the reflectivity one plane at a time, a feat made possible by modern computers. As this allows the structure, composition and position of each plane to be specified, it has previously proved useful for dynamical diffraction calculations on strained crystals, heterostructures, surface structures and even quasicrystals (Durbin & Follis, 1995; Chung & Durbin, 1995).

2. Darwin theory with phonon modes

In our numerical simulations of X-ray reflectivity, we model Si and Ge crystals consisting of 300 000 (110) atomic planes. We use the extended Darwin theory of dynamical X-ray diffraction, which differs from the original (Darwin, 1914) only in that the reflectivity of each plane is computed numerically and is then employed in the Darwin recursion relations, instead of using analytical results based on an assumed periodicity.

The Darwin model assumes that the crystal is made up of well defined planes of atoms at well defined positions. The instantaneous set of phonon modes in a crystal will produce a definite displacement for every atom within each plane. What we aim to show in this section is that the reflectivity can be calculated by considering separately the displacements from transverse and longitudinal waves, and by taking into account the projection of the atomic displacements in the direction of the scattering wave vector. The fact that X-ray diffraction is sensitive only to displacements normal to the diffraction planes is an important distinction between diffraction from phonons and general phonon phenomena.

To calculate the Darwin reflectivity in the presence of phonons, it is necessary to map the effect of lattice vibrations onto an equivalent planar displacement. This is trivial for longitudinal phonons parallel to the scattering direction, *i.e.* in the surface normal direction $\hat{\mathbf{z}}$. Here each atomic plane actually does experience a uniform displacement given by

ISSN 0108-7673

$$u_n(\mathbf{K}) = a_{\mathbf{K}} \exp[i(\omega t - Knd - \delta_{\mathbf{K}})], \quad (1)$$

where n is the index plane, $\mathbf{K}$ and ω are the phonon wave vector and frequency and d is the lattice constant. The phonon amplitude is $a_{\mathbf{K}}$, and $\delta_{\mathbf{K}}$ is an arbitrary phase constant. This displacement is used to determine the position of each of the atomic layers and the Darwin algorithm is applied numerically to compute the net reflectivity.

For a transverse wave traveling perpendicular to the scattering direction, the atoms have a sinusoidal pattern of displacements in the z direction:

$$u_n(\mathbf{K}) = a_{\mathbf{K}} \exp[i(\omega_K t - \mathbf{K}_\perp \cdot \mathbf{r}_\perp - \delta_{\mathbf{K}})]. \quad (2)$$

The reflectivity of a single plane with maximum amplitude a and wave vector $\mathbf{K}$ can be computed numerically by going back to Darwin's original Fresnel summation over the scattered spherical waves arriving at the detector from each atom (Darwin, 1914; Warren, 1990; Durbin, 1995). The general expression for scattering by a planar array of atoms at sites $\mathbf{d}_{m_1 m_2} = m_1\mathbf{a}_1 + m_2\mathbf{a}_2$, where $\mathbf{a}_1$ and $\mathbf{a}_2$ are basis vectors, is

$$E = -f(r_e/r)E_o \sum_{m_1,m_2} \exp\{i[k(R_{m_1m_2} + r_{m_1m_2}) - \omega t]\}. \quad (3)$$

Here E is the amplitude at the detector a distance r from the origin, E_o is the amplitude of the incident spherical wave from the source at R, and r_e is the classical electron radius. $R_{m_1m_2}$ and $r_{m_1m_2}$ are the source and detector distances, respectively, for the atom at $\mathbf{d}_{m_1m_2}$. The two summations become Fresnel intervals which give a finite reflectivity for the infinite plane.

The transverse wave gives perpendicular displacements of $\zeta = a\cos(\mathbf{K}\cdot\mathbf{r})$, which leads to a Fresnel sum of the form

$$\sum_{m_1} \exp[ik(C_1 m_1^2 a_1^2 - 2\zeta \sin\theta)], \quad (4)$$

where θ is the angle of incidence and $C_1 = 1/2\sin^2\theta(1/R + 1/r)$ (Chung, 1996; Durbin, 1995). For simplicity, we assume $\mathbf{k}$ and $\mathbf{a}_1$ are coplanar, where $\mathbf{k}$ is the wave vector of the incident wave. This was computed numerically to determine the reflectivity for a single plane, from which the reflectivity of the entire crystal could be calculated. These calculations led to an interesting discovery: for a given maximum displacement normal to the planes, the reflectivity of the crystal was *the same* for a transverse wave as it was for a longitudinal wave.

The equivalence of a parallel longitudinal phonon and a perpendicular transverse phonon is suggested by comparing the instantaneous distribution of atoms about a single plane for the transverse phonon with the instantaneous set of planar displacements from many planes for the longitudinal phonon. These are identical, as shown in Fig. 1, and they produce identical X-ray reflectivities because one configuration can be mapped onto the other by translating atoms by integer multiples of the lattice constant, which leaves the reflectivity unchanged. We can thus replace all perpendicular transverse phonons with parallel longitudinal phonons having the same amplitude; from these the Darwin reflectivity is easily calculated.

This procedure is equivalent to ignoring the correlations among displacements. The scattered intensity from a set of planes would not depend on the ordering of the planes for kinematical diffraction (assuming that absorption effects are negligible). In the Darwin dynamical theory, however, the incident intensity seen by a given plane does depend on the distribution of planes both above and below it, so correlations may be relevant. As the wave-field intensities vary on the scale of the extinction length, one would expect that correlations which vary much faster than that length would have a negligible impact on the overall reflectivity. This is apparently the underlying reason for the above result, that the reflectivity of a crystal is the same for either a longitudinal or a transverse vibrational mode of the same amplitude. Note that all but a tiny fraction of phonon modes have wavelengths much smaller than the extinction length.

Finally, we consider the case of a phonon with arbitrary polarization $\hat{\boldsymbol{\varepsilon}}$ and wave vector $\mathbf{K}$ in any general direction. The z displacement of an atom at position $\mathbf{r}$ on plane n is

$$\begin{aligned} u_n(\mathbf{K}) &= a_K(\hat{\boldsymbol{\varepsilon}}_K \cdot \hat{\mathbf{z}}) \exp[i(\omega_K t - \mathbf{K}_\perp \cdot \mathbf{r}_\perp)] \\ &\quad \times \exp[-i(\delta_K + K_\parallel z)] \\ &= a'_K \exp[i(\omega_K t - \mathbf{K}_\perp \cdot \mathbf{r}_\perp - \delta'_K)]. \end{aligned} \quad (5)$$

Note that the displacement has exactly the same form as (2) for a perpendicular transverse phonon. In other words, a general phonon of amplitude a, polarization $\hat{\boldsymbol{\varepsilon}}_K$ and frequency ω_K produces displacements in a single

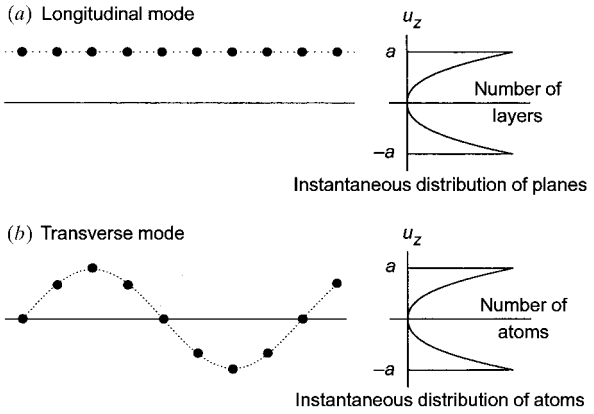

Fig. 1. Instantaneous distributions of the displacements. (*a*) Longitudinal mode with $\mathbf{K} \parallel \hat{\mathbf{z}}$ showing displacements of atoms throughout the crystal. (*b*) Transverse mode with $\mathbf{K} \perp \hat{\mathbf{z}}$ showing displacements of atoms within a single plane. The two cases show identical distributions.

plane equivalent to a perpendicular transverse phonon with amplitude $a(\hat{\boldsymbol{\varepsilon}}_K \cdot \hat{\mathbf{z}})$ and the same frequency. That in turn leads to the same X-ray reflectivity as a parallel longitudinal phonon with the same amplitude and frequency since only displacements in the **z** direction affect the diffracted amplitude. This leads to a powerful simplification: the X-ray reflectivity can be determined by calculating the total displacement of each plane in the crystal by treating every phonon as if it were a parallel longitudinal phonon with the appropriate amplitude.

3. Computational results

To produce a realistic simulation of temperature-dependent diffraction, we utilized standard phonon-dispersion relations measured by inelastic neutron diffraction to determine $\omega_{\mathbf{K}}$ *versus* $\mathbf{K}$ (Nilsson & Nelin, 1971). To simplify the calculation, we assumed isotropic dispersion curves, selecting the [001] data to represent all directions in the Brillouin zone. The amplitude of each phonon is derived by thermodynamic arguments as

$$\langle a_{\mathbf{K}}^2 \rangle = 2[n(T) + 1/2]\hbar/Nm\omega_{\mathbf{K}}, \qquad (6)$$

where $\hbar$ is Planck's constant, m is the atomic mass and N is the total number of atoms in the crystal (Warren, 1990). The effect of temperature on the X-ray reflectivity enters this calculation only through the Bose–Einstein distribution function, $n(T)$, which gives the occupation number for each phonon. (We assume throughout that all lattice vibrations are purely harmonic. While contributions from anharmonic effects are crucial for many real materials, it is the intent of this work first to understand better the harmonic crystal.)

Finally, the sum over all phonon modes is simplified by dividing the Brillouin zone into $16^3 = 4096$ discrete cells, and representing all phonons within each cell by the amplitude at the center of the cell. The number of computational cells was chosen by observing that a larger number produced no change in the results. Since the phonons nearer the zone center have larger amplitudes and hence play a greater role in affecting diffraction, having a smaller cell size close to the zone center proved to be computationally more efficient. The final parameter is the phase δ_K for each phonon; these were selected by a random-number generator.

A reflectivity calculation for a given temperature begins by adding the displacements from all phonons to determine the position of each of the 300 000 planes. (As already noted, all phonons were treated as parallel longitudinal phonons.) From this fixed configuration, the reflectivity curves were computed for the 220, 440, 660 and 880 reflections. The integrated intensities of these Darwin curves correspond to the X-ray reflectivity for each reflection; this can then be plotted *versus* temperature and compared to the Debye theory.

A physical measurement of crystal reflectivity must actually correspond to some kind of an average over atomic displacements, whereas the calculation described so far would be the reflectivity from a particular fixed configuration of displacements. To make this simulation more realistic, it must sample many configurations of the crystal. One approach would be to repeat it many times with new values for the random phonon phases δ_K, since each set is a new configuration. As this proved to be extremely demanding of computer time, we instead performed a single calculation of the planar displacements, but with a new set of random phases δ_K for each of the 300 000 planes. The resultant distribution closely matched the average of the limited number of individual configurations which were computed, and the reflectivity also agreed with the averages, so we conclude that this is a fair and more efficient manner for configurational averaging.

The first task is to check whether this method is consistent with experimental results and with standard Debye theory over a range of temperatures. Proper accounting of the Bose–Einstein distribution function leads to a temperature dependence of the Debye–Waller factor M which includes the Debye function $\Phi(T_D/T)$:

$$M = (6h^2T/mkT_D^2)[\Phi(x) + x/4](\sin\theta/\lambda)^2,$$

where $x = T_D/T$ and T_D is the Debye temperature (Warren, 1990). The Debye function is $\Phi(x) = (1/x)\int_0^x \xi/(e^\xi - 1)\,\mathrm{d}\xi$. We follow conventional practice and plot the log of the diffracted intensity *versus* the product of temperature T and the dimensionless function $[\Phi(x) + x/4]$ since this yields a straight line with the Debye theory. Fig. 2 shows a comparison of Batterman's measurements of the Si 660 reflection (Batterman, 1962), his fit to the Debye theory and our Darwin calculations. The agreement is excellent, especially considering that the Debye theory uses the Debye temperature as a fitting parameter whereas the Darwin theory is essentially parameter-free.

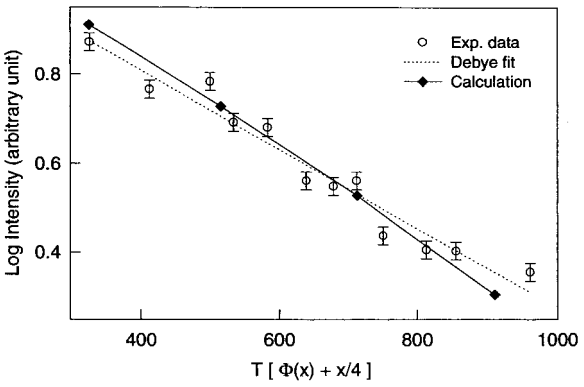

Fig. 2. The log intensity *versus* $T[\Phi(x) + x/4]$ for the Si 660 reflection. Here $\Phi(x) = (1/x)\int_0^x \xi/(e^\xi - 1)\,\mathrm{d}\xi$ and $x = T_D/T$, where T_D is the Debye temperature. The circles denote the experimental data and the diamonds represent the Darwin calculations. The dotted line is a straight-line fit from which the Debye temperature was determined.

Next we investigated this Darwin model over a wider range of temperatures and a range of scattering wave vectors. Fig. 3 shows the computed Darwin reflectivities for Ge 220, 440, 660 and 880 reflections from 5 to 900 K, along with the Debye theory predictions. The Debye–Waller factor was determined from the computed width of the distribution of atomic planes at each temperature, which proved to be Gaussian for even the highest temperatures. Agreement between the Darwin calculation and the Debye theory is good at low temperatures and for low-order reflections but the deviations become large at high temperatures and higher orders.

Debye theory basically assumes that all X-rays see the same crystal, *i.e.* that corresponding to the time-averaged charge distribution of each atom. The Darwin calculation is effectively the average of the reflectivities from many different instantaneous configurations. We argue below that a physical measurement is more like the Darwin calculation than the Debye theory. The discrepancy in Fig. 3 is therefore the first indication that a real reflectivity measurement may not be consistent with the Debye average-crystal model. We note that these deviations at higher temperatures cannot be simply the consequence of larger displacements because the calculations still show the Gaussian profile for the distribution of planar displacements required for the validity of the Debye–Waller factor. Correlations between planes also cannot play any role since, as previously noted, a new set of random phonon phases is used in calculating the reflectivity of each successive plane.

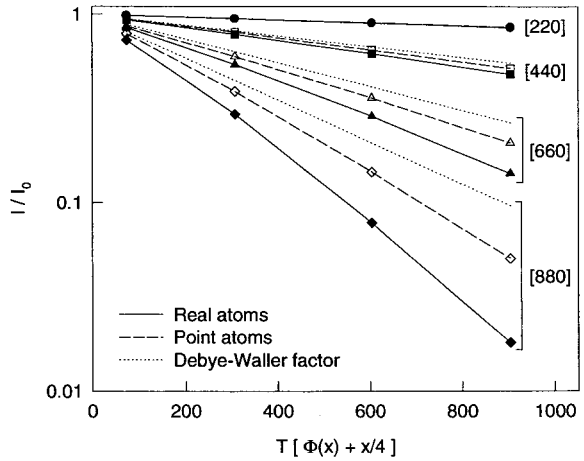

Fig. 3. The calculated log intensity *versus* $T[\Phi(x) + x/4]$ for Ge reflections. [The role of the dimensionless Debye function $\Phi(x)$ is noted in the text.] The solid lines represent real atoms including the form-factor corrections for the finite atomic size, the dashed lines are for point atoms (without form factors) and the dotted lines are the predictions from the Debye–Waller factor. The Darwin calculations show large deviations from the Debye theory at high temperatures and for higher-order reflections. The deviations are smaller for the point atoms.

As a result of the sensitivity to larger scattering wave vectors, we were interested in testing whether the finite size of the scattering atoms might be playing a role. We repeated the calculations without using the form-factor corrections to the Ge atomic scattering factor, which is equivalent to shrinking the real Ge atom down to a point. These results, also plotted in Fig. 3, show much weaker deviations from the Debye theory. This suggests that atomic size might indeed play a role in the temperature dependence of X-ray reflectivity.

These unexpected results raise the question of whether some kind of transition from dynamical to kinematic diffraction might be at work. By fitting each reflectivity calculation to $I = I_o \exp(-\alpha M)$, these results can be replotted as α *versus* the relative mean atomic displacement, $\langle u^2\rangle^{1/2}/d_{hkl}$, as shown in Fig. 4. Note that standard dynamical theory assumes a constant $\alpha = 1$ while kinematic theory has $\alpha = 2$. Clearly the results are not constant, and only approach unity for the lowest-order reflections at low temperatures. Fig. 4 also shows α plotted against an effective displacement u', which combines the atomic displacements with an atomic size, $u' \equiv (u^2 + \delta u^2)^{1/2}$. The data cluster about a single line when $\delta u = 0.25$ Å, which can be compared to the ionic radius of 0.53 Å for Ge^{4+}. While these results are not understood, they do cast doubt on the rigorous applicability of the standard $\exp(-M)$ temperature dependence ascribed to dynamic diffraction.

To investigate further whether these data represent a crossover effect from dynamical to kinematic behavior, we have extracted the minimum extinction lengths from the calculations and compared them to the absorption length to give an indicator of how dynamical the scat-

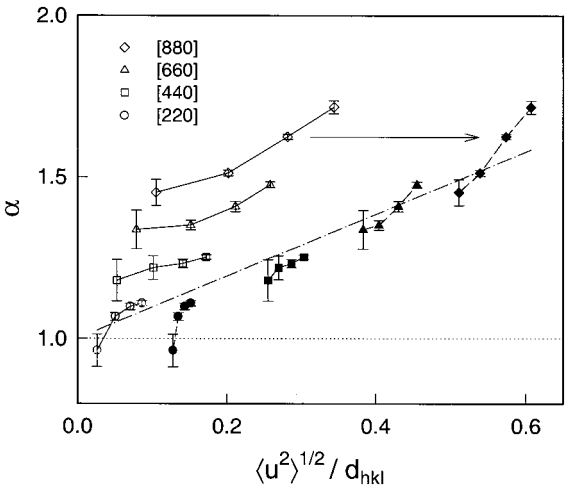

Fig. 4. The values of α *versus* $\langle u^2\rangle^{1/2}/d_{hkl}$. The solid symbol used $\langle u'^2\rangle^{1/2}/d_{hkl}$ as x values, where $u'^2 = u^2 + \delta u^2$, which adds an effective ionic size to the vibrational amplitudes to simulate the total charge distribution. The data tend to cluster about the dashed line when $\delta u = 0.25$ Å. The dotted line is the prediction of standard dynamical theory.

tering is. Even at 900 K for the 880 Ge reflection, the extinction length is only 0.86 times the absorption length although α is nearly 1.8. This indicates that diffraction is still very much in the dynamical regime, but it would be hard to quantify how the Debye–Waller factor should behave in the transition region between dynamical and kinematic diffraction. The extended Darwin theory used here would still be correct in the kinematic region as long as the crystal can be modeled as a set of parallel planes.

4. Deviations from Debye and the ergodic hypothesis

The Debye model assumes X-rays scatter off the time-averaged charge distribution (Debye, 1914; Waller, 1923), while the Darwin calculations compute the reflectivities of many configurations first and then take the average. The limit in which these two are equivalent is described as 'quasi-ergodicity' by Zachariasen (1994). The discrepancies observed here may indicate a lack of ergodicity in dynamical diffraction.

The central issue here is whether a physical diffraction measurement effectively samples a crystal for a time that is long or short compared to phonon time scales, *i.e.* around 10^{-12} s. We first note that the period of oscillation for a 10 keV photon is less than 10^{-18} s, a fact that in itself led Zachariasen to conclude that 'the scattering of X-rays represents interaction with the instantaneous structure' (Zachariasen, 1994, p. 176). Perhaps more relevant is the coherence time of an X-ray wave train which follows from the uncertainty principle, $\Delta E \times \Delta t > \hbar$. For a typical energy width of 3 eV, this coherence time is about 10^{-16} s. (This number is of the same order for synchrotron X-rays monochromated by standard Si crystals, for example, as well as for characteristic Cu $K\alpha$ fluorescence X-rays.) Another characteristic time scale is that for a photon traversing a thickness of crystal encountered in diffraction, which is of the order of 10^{-14} s for a 10 μm extinction length. All of these physical time scales are much shorter than the time required for significant changes in atomic displacements. For this reason, we claim that a diffracted signal of N photons corresponds to reflections from N different instantaneous atomic configurations. Thus, a physical measurement is more like the Darwin than the Debye model.

Can the scattering from an instantaneous configuration be significantly different from the average crystal? Even when a large number of phonon modes is included in the model, the Darwin calculations show that the average can be very different from the instantaneous. A simple example for a single phonon shows how this is possible. Consider a crystal made up of identical atomic planes with interplanar spacing a_o. If we choose a unit cell of length $2a_o$ in the direction normal to the planes, the structure factor for the fundamental reflection in the [00l] direction is $F_{002} = 2f$ and F_{001} is identically zero (f is the atomic scattering factor). Now consider a simple longitudinal vibration where successive planes are displaced by $+a\cos\omega t$ and $-a\cos\omega t$, *i.e.* a zone-boundary longitudinal phonon. This alternating expansion and contraction of the interplanar spacing doubles the fundamental periodicity, $2a_o$. A straightforward calculation gives $\langle F_{002}^2\rangle = 2f^2[1 + J_o(4\pi a/a_o)]$ and $\langle F_{001}^2\rangle = 2f_1^2[1 - J_o(2\pi a/a_o)]$ where the angle brackets denote time averaging and J_o is the Bessel function of zero order. On the other hand, the Fourier transform of the time-averaged charge density yields $F_{002}^2 = [2fJ_o(2\pi a/a_o)]^2$ and $F_{001}^2 = 0$. That is, the scattering from the time-averaged crystal is identically zero for the 001 reflection while the average of all the instantaneous scattering is finite. These results are illustrated in Fig. 5.

5. Conclusions

Darwin calculations of perfect-crystal reflectivity, which include phonon vibrations but without assuming the Debye average-crystal model, produce results in good agreement with the expected $\exp(-M)$ behavior for relatively low temperatures and low-order reflections in Si and Ge. However, the computed reflectivities differ significantly from Debye values for high temperatures and high-order reflections. The finite size of the atoms is a notable factor in the temperature dependence. While

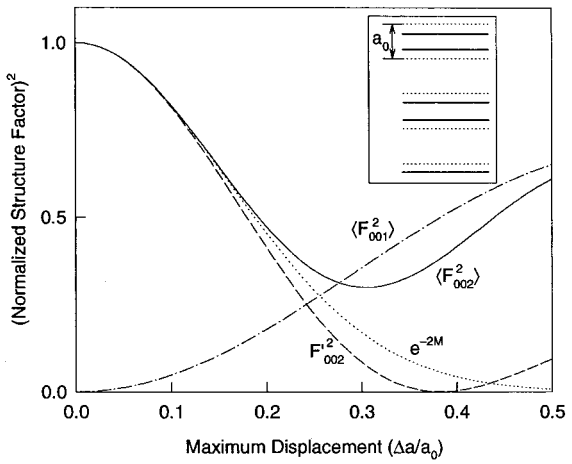

Fig. 5. Difference in structure factors for a single longitudinal vibration where successive planes are displaced by $+a\cos\omega t$ and $-a\cos\omega t$. The brackets denote time averaging, and F' is from the Fourier transform of the time-averaged charge distribution. The dotted line shows the corresponding Debye–Waller factor $\exp(-2M)$. Not shown is the structure factor for scattering from the 001 Fourier component of the average crystal, which is identically zero ($F' = 0$); the time average of the scatttering from the instantaneous 001 Fourier component of the crystal is non-zero for all finite values of the amplitude. (Note that a maximum displacement of 0.5 is unphysically large; the difference between the instantaneous and the time-averaged crystal persists down to small amplitudes, however.) The inset shows the displacements of atomic layers (solid line) from their equilibrium positions (dotted line).

in real crystals there are various effects, such as anharmonicity, which might also cause deviations from the simple Debye model we consider here, there was previously no reason to question the applicability of the Debye model for dynamical diffraction in ideal systems. An understanding of these differences could be important for interpreting the temperature dependence of X-ray diffraction from Si, Ge and various MBE-grown heterostructures which diffract dynamically.

References

Batterman, B. W. (1962). *Phys. Rev.* **127**, 686–690.

Batterman, B. W. & Cole, H. (1964). *Rev. Mod. Phys.* **36**, 681–717.

Chung, J.-S. (1996). PhD thesis, Purdue University, West Lafayette, IN, USA. Unpublished.

Chung, J.-S. & Durbin, S. M. (1995). *Phys. Rev. B*, **51**, 14976–14979.

Darwin, C. G. (1914). *Philos. Mag.* **27**, 315–333, 675–690.

Debye, P. (1914). *Ann. Phys.* **43**, 49–95.

Durbin, S. M. (1995). *Acta Cryst.* A**51**, 258–268.

Durbin, S. M. & Follis, G. C. (1995). *Phys. Rev. B*, **51**, 10127–10133.

James, R. W. (1950). *Optical Principles of the Diffraction of X-rays.* In *The Crystalline State*, Vol. 2, edited by Sir L. Bragg. London: G. Bell & Sons.

Nilsson, G. & Nelin, G. (1971). *Phys. Rev. B*, **3**, 364–369.

Ohtsuki, Y. H. (1964). *J. Phys. Soc. Jpn*, **19**, 2285–2292.

Parthasarathy, R. (1960). *Acta Cryst.* **13**, 802–806.

Waller, I. (1923). *Z. Phys.* **17**, 398–408.

Warren, B. E. (1990). *X-ray Diffraction*, chs. 3 and 11. New York: Dover.

Zachariasen, W. H. (1994). *Theory of X-ray Diffraction in Crystals*, ch. 4. New York: Dover.